Publications of the Astronomical Society of the Pacific, **116**:391–396, 2004 May

A Far-Ultraviolet Spectroscopic Analysis of the Central Star of the Planetary Nebula Longmore 1[1]

J. E. Herald and L. Bianchi

Department of Physics and Astronomy, Johns Hopkins University, 3400 North Charles Street, Baltimore, MD 21218-2411; herald@pha.jhu.edu, bianchi@pha.jhu.edu

Received 2004 January 18; accepted 2004 February 20; published 2004 April 20

ABSTRACT. We have performed a non-LTE spectroscopic analysis using far-UV and UV data of the central star of the planetary nebula K1-26 (Longmore 1) and found $T_{\rm eff} = 120 \pm 10$ kK, $\log g = 6.7^{+0.3}_{-0.7}$ cm s^{-2}, and $Y \simeq 0.10$. The temperature is significantly hotter than previous results based on optical line analyses, highlighting the importance of analyzing the spectra of such hot objects at shorter wavelengths. The spectra show metal lines (from, e.g., carbon, oxygen, sulfur, and iron). The signatures of most elements can be fit adequately using solar abundances, confirming the classification of Lo 1 as a high-gravity O(H) object. Adopting a distance of 800 pc, we derive $R_* \simeq 0.04\ R_\odot$, $L \simeq 250\ L_\odot$, and $M \simeq 0.6\ M_\odot$. This places the object on the white dwarf cooling sequence of the evolutionary tracks with an age of $\tau_{\rm evol} \simeq 65$ kyr.

1. INTRODUCTION

Longmore 1 (K1-26, PK 255−59°1, hereafter Lo 1) was originally discovered by Longmore (1977) as a planetary nebula (PN) having a notably large angular size (∼400″). The spectra of its central star show both hydrogen and He II absorption features, with no evidence of a stellar wind in its UV or optical spectra (Patriarchi & Perinotto 1991; Kaler & Lutz 1985; Mèndez et al. 1985). Because of its high Galactic latitude ($b \simeq -60°$), the reddening toward Lo 1 is thought to be minimal (Kaler & Lutz 1985). Based on its optical spectrum, Mèndez et al. (1985) termed Lo 1 an "hgO(H)" star, a high-gravity object with very broad Balmer absorptions. Such objects can lie on the white dwarf cooling tracks, but can also be non-post-AGB objects. A distance of $D = 800$ pc (Ishida & Weinberger 1987) implies a nebular radius of ∼0.8 pc, suggesting that Lo 1 is a quite evolved central star of the planetary nebulae (CSPN; most PNs have radii ≲0.5 pc; Cahn et al. 1992).

Hot CSPNs emit most of their observable flux in the far-UV range. We have observed the central star of Lo 1 with the *Far Ultraviolet Spectroscopic Explorer* (*FUSE*) satellite in the 905–1187 Å range. Using this data, as well as archive *International Ultraviolet Explorer* (*IUE*) data (1150–3300 Å), we determined the parameters of the central star through stellar modeling and discuss evolutionary implications.

Parameters of Lo 1 compiled from previous literature are listed in Table 1.

[1] Based on observations made with the NASA-CNES-CSA *Far Ultraviolet Spectroscopic Explorer* and data from the MAST archive. *FUSE* is operated for NASA by the Johns Hopkins University under NASA contract NAS 5-32985.

2. OBSERVATIONS AND REDUCTION

Table 2 lists the spectra utilized in this paper. Lo 1 was observed as part of *FUSE*'s Cycle 1 program P133 (Bianchi). The *IUE* data were retrieved from the MAST archive. The observed spectra are presented in § 3.

FUSE covers the wavelength range of 905–1187 Å at a spectral resolution of ≲30,000. The flux calibration accuracy of *FUSE* is ≲10% (Sahnow et al. 2000). It is described by Moos et al. (2000), and its on-orbit performance is discussed by Sahnow et al. (2000). *FUSE* collects light concurrently in four different channels (LiF1, LiF2, SiC1, and SiC2). Each channel is recorded by two detectors, each divided into two segments (A and B) covering different subsets of the above range with some overlap.

The *FUSE* spectra were taken through the LWRS (30″ × 30″) aperture. These data, taken in "time tag" mode, have been calibrated using the most recent *FUSE* data reduction pipeline, efficiency curves and wavelength solutions (CALFUSE ver. 2.2). We combined the data from different segments, weighted by detector sensitivity, and rebinning to a uniform dispersion of 0.05 Å (which is probably close to the actual resolution, since the data were taken in the early part of the mission). Bad areas of the detectors, and those regimes affected by an instrumental artifact known as "the worm" (*FUSE* Data Handbook ver. 1.1), were excluded. For part of the first observation, telescope alignment problems moved the target out of the LiF2/SiC2 aperture. This also appears to have happened with the SiC2 detector halfway through the second observation. We thus omitted data taken during these target drifts for the affected detectors.

Four *IUE* spectra of the central star of Lo 1 are available;

TABLE 1
Parameters of Lo 1

Quantity	Value	References/Notes
R.A. (J2000)	02 56 58.23	…
Decl. (J2000)	−40 10 19.41	…
Galactic latitude, b (deg)	−59.64	1
Galactic longitude, l (deg)	255.35	1
Height, z (pc)	−690	1
Lateral distance, q (pc)	400	1
Radial distance, D (pc)	800	1
PN radius R_{PN} (arcsec)	187, 230 × 192	2
PN radius R_{PN} (pc)	0.72, 0.89 × 0.75	Assuming $D = 800$ pc
v_{rad} (km s^{-1})	65 ± 21	3
Logarithmic extinction at Hβ,c	0.0 ± 0.05	4
CSPN V (mag)	15.4	5
CSPN T_{eff} (kK)	65 ± 10	6
CSPN log g (cm s^{-2})	5.7 ± 0.3	6
CSPN He/H	0.1 ± 0.03	6

Note.—Units of right ascension are hours, minutes, and seconds, and units of declination are degrees, arcminutes, and arcseconds.

References.—(1) Ishida & Weinberger 1987; (2) Longmore 1977 and Kohoutek & Laustsen 1977; (3) West & Kohoutek 1985; (4) Kaler & Feibelman 1985; (5) Kaler & Lutz 1985; (6) Mèndez et al. 1985, from optical analysis.

however, it appears that one (SWP20275) missed the central star. The only high-resolution spectrum (SWP39146) is underexposed and was not used. The two remaining low-resolution long-wavelength and short-wavelength spectra are in agreement in the region of overlap. The *IUE* spectra are relatively featureless and are mainly used to fit the continuum flux distribution.

3. MODELING

Modeling of Lo 1 consisted of two parts: modeling the hot central star and modeling the sight-line hydrogen (atomic and molecular). We describe each in turn. A virtue of its location significantly outside the Galactic plane is a low reddening, which we determine, by fitting the continuum slope, to be $E_{B-V} < 0.01$ (we use a value of $E_{B-V} = 0$ throughout this paper). The data, as well as the model fits, are shown in Figures 1 and 2. We determine the radial velocity of Lo 1 to be $v_{rad} = 100 \pm 10$ km s^{-1} using stellar absorption line features in the long wavelength *FUSE* range (>1050 Å) such as C IV λ1169.0 and C IV λ1107.6.

TABLE 2
Lo 1: Utilized Spectra

Instrument	Data Set	Date	Resolution (Å)	Aperture (arcsec)
FUSE	P1330601001	2000 Dec 11	∼0.05	30 × 30
FUSE	P1330601002	2000 Dec 11	∼0.05	30 × 30
IUE	LWP11432	1987 Aug 19	5–6	10 × 20
IUE	SWP21421	1983 Nov 1	5–6	10 × 20

3.1. The Central Star Model

To model the white dwarf central star, we used the TLUSTY code to calculate the stellar atmosphere, and SYNSPEC to calculate the synthetic flux (Hubeny 1988; Hubeny & Lanz 1992, 1995; Hubeny et al. 1994). TLUSTY calculates the atmospheric structure assuming radiative and hydrostatic equilibrium, and a plane-parallel geometry, in non-LTE (NLTE) conditions. In the case of hot ($T_{eff} \gtrsim 50$ kK) white dwarfs, LTE calculations are not appropriate and result in significant deviations from NLTE calculations (see, e.g., Dreizler & Werner 1996; Werner 1996; Werner et al. 1991; Napiwotzki 1997). This is because in such hot objects, the populations of the ions are mainly determined by the intense radiation field despite the high gravities.

The *FUSE* spectrum shows features of hydrogen, helium, and metals (e.g., C, O, Fe, and S), with O VI λλ1032, 1038 being especially prominent. Test models indicated that the solar abundance ratio for H/He (as found by Mèndez et al. 1985) was adequate. We thus constructed a grid of solar abundance models varying T_{eff} and log g, treating hydrogen and helium in NLTE to calculate the structure of the atmosphere. Once T_{eff} and log g were determined adequately, they were held fixed, and the CNO elements were varied individually in NLTE to constrain their abundances and ensure that neglect of their NLTE treatment did not alter the derived T_{eff} and log g.

The atomic data used come from TOPBASE, the database of the Opacity Project (Cunto et al. 1993). TLUSTY makes use of the concept of "superlevels," where levels of similar energy are grouped together and treated as a single level in the rate equations (after Anderson 1989). The number of levels

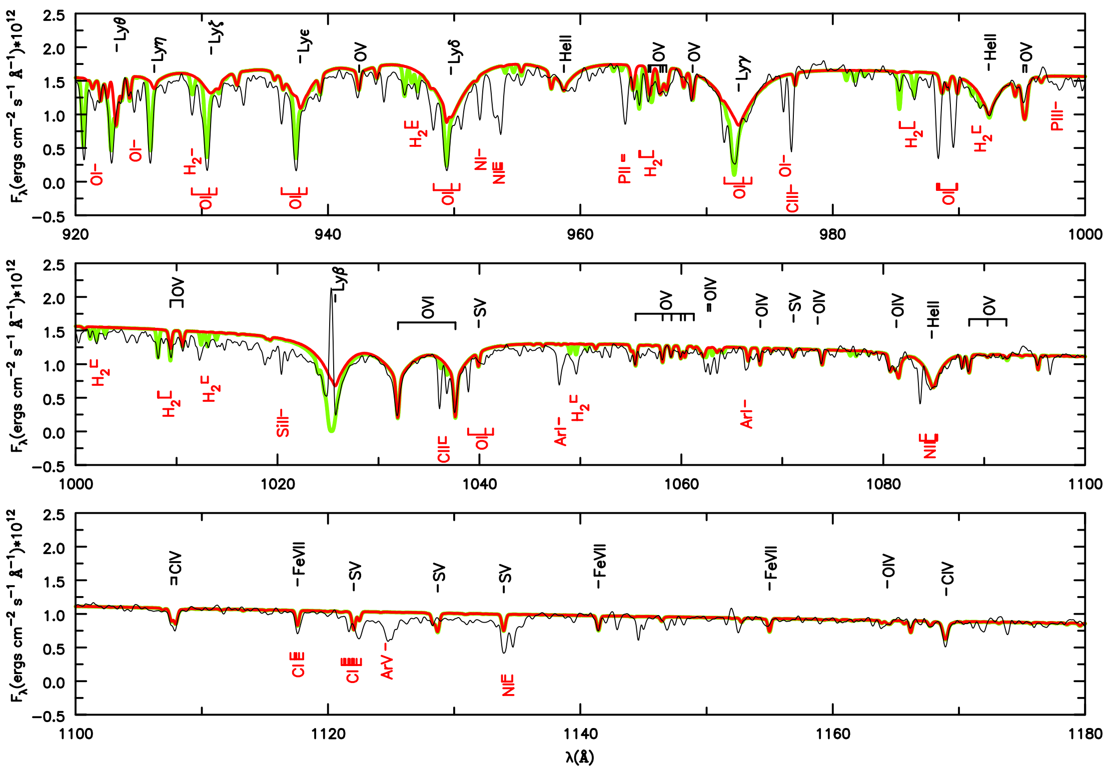

FIG. 1.—FUV *FUSE* spectrum of Lo 1 (*black*), along with our stellar model (described in § 3.1), both with (*light gray*) and without (*dark gray*) our hydrogen absorption model applied. Prominent stellar features are marked with black labels, interstellar absorption features and airglow lines with gray labels. The Lyman features consist of a broader, stellar component and a narrower, interstellar component separated by ≃100 km s^{-1} in velocity space (the Lyβ emission is airglow). All spectra have been convolved with a Gaussian of 0.25 Å for clarity. Virtually all the stellar and hydrogen features are well matched; most nonmatched features are of interstellar origin. [*See the electronic edition of the PASP for a color version of this figure*.]

+superlevels used for the NLTE model ions were H I (8+1), He I (24+0), He II (20+0), C III (34+12), C IV (35+2), N IV (15+8), N V (21+4), O IV (39+31), O V (34+6), and O VI (15+5). Ne, Na, Mg, Si, S, Ar, Ca, and Fe were allowed to contribute to the total number of particles and charge, but their opacity contribution was neglected in the model atmosphere calculation. We have adopted SYNSPEC's values for solar abundances, which are taken from Grevesse & Sauval (1998).

As previously mentioned, a solar hydrogen-to-helium ratio appeared adequate to fit the He II and H Lyman spectrum. The gravity was constrained by fitting mainly the wings of these features, as demonstrated in Figure 3. To determine the effective temperature, the FUV–UV continuum shape, as well as FUV spectral features of hydrogen, helium and metals (mainly oxygen and carbon), were used as diagnostics. The parameters of our best-fit model for the CSPN of Lo 1 are $T_{\rm eff}$ =

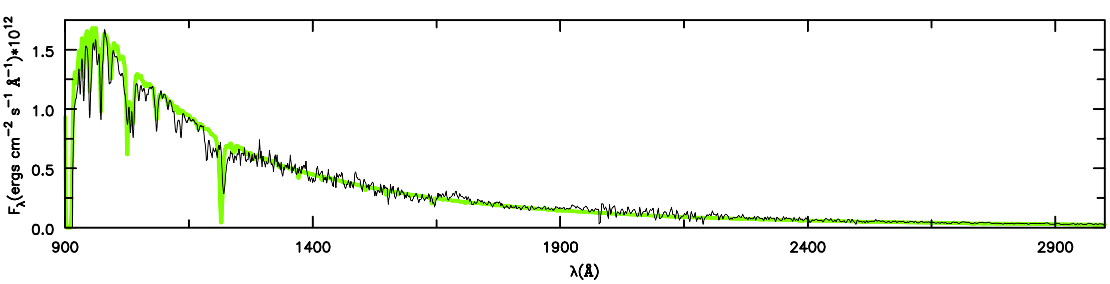

FIG. 2.—FUV–UV (*FUSE* and *IUE*) spectra of Lo 1 (*black*), along with our stellar models (*dark gray*) with our hydrogen absorption model applied (convolved with a 3 Å Gaussian). The model, with no reddening applied, does a good job at matching the observed flux distribution. [*See the electronic edition of the PASP for a color version of this figure*.]

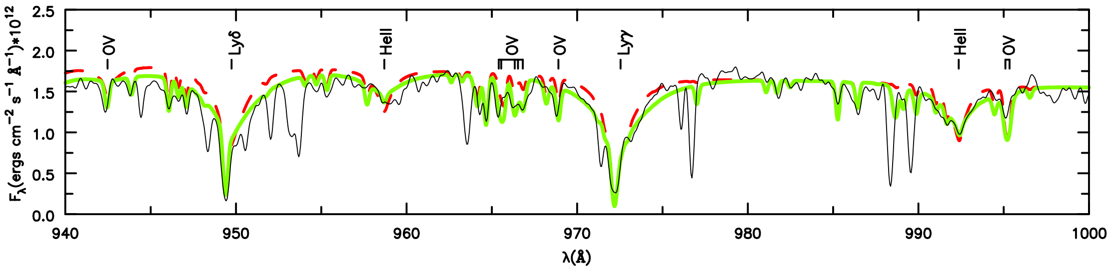

FIG. 3.—Constraining the gravity: Portion of the *FUSE* spectrum (*black*), along with our stellar model ($T_{\rm eff} = 120$ kK), with $\log g = 6.0$ cm s^{-2} (*dashed dark gray*) and $\log g = 7.0$ cm s^{-2} (*solid light gray*). Based on the wings of the Lyδ, Lyγ, and the He II features, the gravity lies between these two values. We derive $\log g = 6.7^{+0.3}_{-0.7}$ cm s^{-2}. [*See the electronic edition of the PASP for a color version of this figure*.]

120 ± 10 kK, $\log g = 6.7^{+0.3}_{-0.7}$ cm s^{-2}. Solar values for the metal abundances were found to be adequate, except for oxygen, for which the solar value underproduced the strong O VI λλ1032, 1038 feature (shown in Fig. 4). We found that an oxygen abundance enriched 5 times with respect to the solar value ($X_{\rm O} = 5\,X_\odot$ by mass) produced a good fit; however, some of the other oxygen features then appeared a bit strong. For temperatures $T_{\rm eff} \simeq 100 - 120$ kK, the O VI feature is at its strongest, thus higher or lower temperatures require an even greater oxygen enrichment. Unless otherwise stated, the model spectrum shown in the figures and what we refer to as "our model" has the parameters $T_{\rm eff} = 120$ kK, $\log g = 6.7$ cm s^{-2},

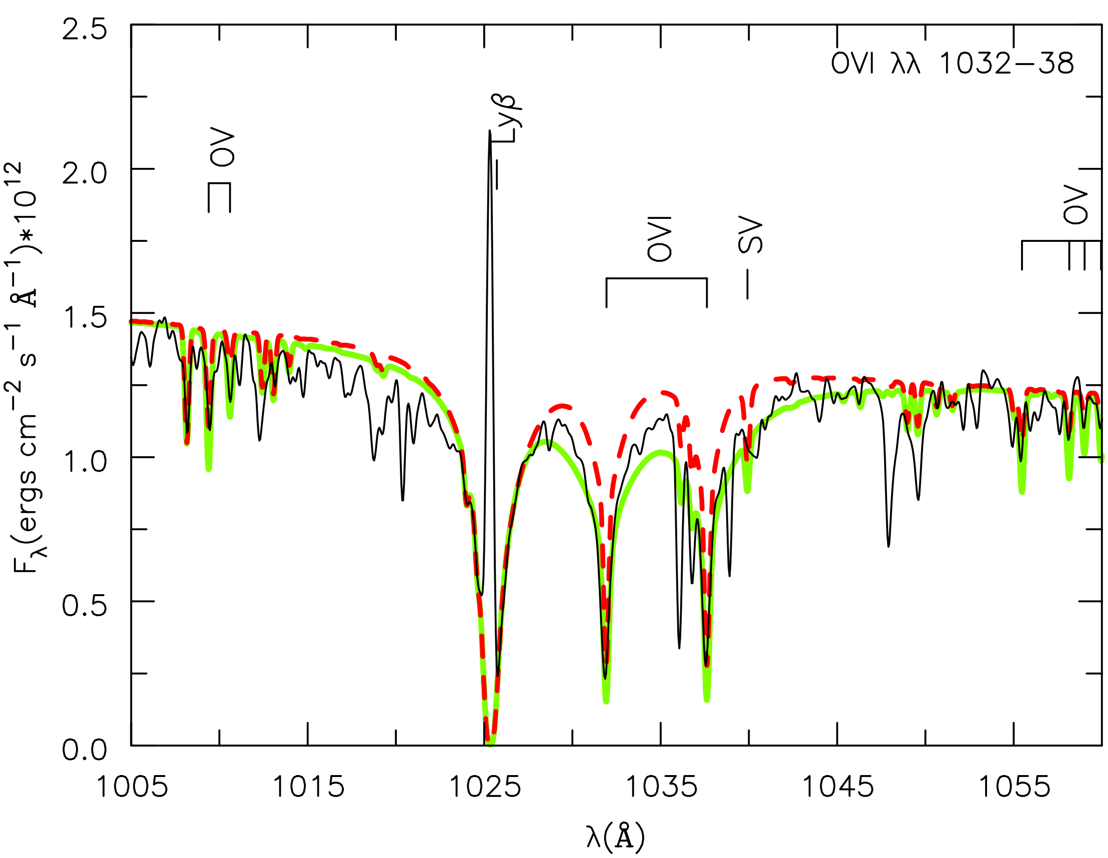

FIG. 4.—Constraining the oxygen abundance: *FUSE* spectrum in the region of O VI λλ1032, 1038 (*black*), along with a stellar model with solar oxygen abundance (*dashed dark gray*) and a model with oxygen enriched 10 times with respect to the solar value (*solid light gray*). The former underproduces the O VI doublet, while the latter overproduces the feature. Our final model, with an oxygen abundance of 5 times the solar value, fits the O VI doublet well (shown in Fig. 1). [*See the electronic edition of the PASP for a color version of this figure*.]

TABLE 3
DERIVED PARAMETERS FOR LO 1

Parameter	Value	Primary Diagnostics and Comments
CSPN $T_{\rm eff}$ (kK)	120 ± 10	H Lyζ–Lyβ, He II, metal features
CSPN log g (cm s^{-2})	$6.70^{+0.3}_{-0.4}$	H Lyζ–Lyβ, He II wings
CSPN R_*/D ($R_\odot$ pc^{-1})	$(4.6 \pm 0.3) \times 10^{-5}$	Scaling model flux to observed UV flux
CSPN $X_{\rm O}$ ($X_\odot$)	1–5	O VI λλ 1032, 1038, other oxygen features
CSPN R_* ($R_\odot$)	$(3.7 \pm 0.2) \times 10^{-2}$	Using D = 800 pc
CSPN L ($L_\odot$)	250^{+140}_{-100}	…
E_{B-V} (mag)	<0.01	Continuum shape
Interstellar log N(H I) (cm^{-2})	$20.3^{+0.4}_{-0.3}$	Lyman features, T = 80 K assumed
Interstellar log $N(H_2)$ (cm^{-2})	14.9 ± 0.2	FUV H_2 features, T = 80 K assumed
$V_{\rm rad}$ (km s^{-1})	−100 ± 10	Photospheric absorption lines

$X_{\rm O} = 5\ X_\odot$, with the abundances of all other elements set to their solar values.

3.2. Modeling H_2 and H I Absorption Toward Lo 1

The *FUSE* spectrum of Lo 1 (Fig. 1) displays a series of absorption features corresponding to the hydrogen Lyman sequence. The cores of these features are attributable to absorption from sight-line hydrogen. These cores are velocity shifted with respect to the broader, stellar Lyman absorption features by ≃100 km s^{-1}, which corresponds to our measured radial velocity for the CSPN lines. Thus, these features are interstellar in origin (rather than circumstellar).

The effects of H I absorption were applied to the model spectrum in the following manner. For a given column density (N) and gas temperature (T), the absorption profile of each line is calculated by multiplying the line core optical depth (τ_0) by the Voigt profile [$H(a, x)$], where x is the frequency in Doppler units and a is the ratio of the line damping constant to the Doppler width (the "b" parameter). The observed flux is then $F_{\rm obs} = \exp\,[-\tau_0 {\rm H}(a, x)] \times F_{\rm intrinsic}$.

Because the H I column density determination is insensitive to temperature, we determine N(H I) by assuming T(H I) = 80 K (corresponding to the mean temperature of the ISM; Hughes et al. 1971) and $v_{\rm turb} = 10$ km s^{-1} and fitting the Lyman profiles of the *FUSE* data. Doing so, we derive log N(H I) = $20.3^{+0.4}_{-0.3}$ cm^{-2}.

The *FUSE* spectrum also shows some weak absorption features from intervening molecular hydrogen, which originate from the Lyman ($B^1\Sigma_u^+$–$X^1\Sigma_g^+$) and Werner ($C^1\Pi_u^\pm$–$X^1\Sigma_g^+$) sequences (these are marked in Fig. 1). We applied the effects of different H_2 models in a similar manner as the H I, again assuming a gas temperature of 80 K. We derive a relatively small column density of log $N(H_2) = 14.9 \pm 0.2$ cm^{-2}. The low column density is probably a consequence of the high Galactic latitude of Lo 1 and is consistent with our determination of $E_{B-V} < 0.01$ mag, based on typical relations between E_{B-V} and H_2 column densities in the ISM found by Bohlin et al. (1978).

Our stellar model spectrum, with hydrogen absorptions corresponding to log N(H I) = 20.3 cm^{-2} and log $N(H_2)$ = 14.9 cm^{-2} applied, is shown in Figure 1.

4. DISCUSSION

Our derived model parameters for the central star and sight-line hydrogen are presented in Table 3. Scaling our model flux to the observed flux yields R_*/D, the ratio of the stellar radius to the distance. This value, using a distance of D = 800 pc (Ishida & Weinberger 1987), yields a radius of $R_* \simeq 0.037\ R_\odot$ and a corresponding luminosity of $L \simeq 250\ L_\odot$. The model flux then yields a corresponding visual magnitude of V = 15.5 mag, in good agreement with the measured value of V = 15.4 mag (Kaler & Lutz 1985). Because we can only constrain the gravity rather loosely, we cannot derive a meaningful value for the mass of the central star without appealing to stellar evolution tracks. As discussed in § 3.1, the O VI doublet may indicate an oxygen enriched atmosphere. Usually, in CSPN, oxygen enrichment is associated with helium-rich objects (i.e., helium burners) and is often accompanied by carbon enrichment. However, the abundances of the other elements in Lo 1 do not appear to be much different than the solar values, which is characteristic of many H-burning CSPN. Therefore, we compared our derived effective temperature and luminosity with both the hydrogen- and helium-burning (solar abundance) tracks of Vassiliadis & Wood (1994). The H-burning tracks indicate a current core mass of $M_c = 0.633\ M_\odot$, and an initial mass of 2.0 $M_\odot$, with the uncertainties of our parameters encompassing the $M_{\rm init} = 1.5\ M_\odot$, $M_c = 0.597\ M_\odot$ and $M_{\rm init}$ = 2.5 $M_\odot$, $M_c = 0.677\ M_\odot$ tracks as well. So, from the H-burning evolutionary models, we derive $M_{\rm init} = 2.0 \pm 0.5\ M_\odot$, $M_c = 0.63 \pm 0.04\ M_\odot$, and a post-AGB age $\tau_{\rm evol} \sim 60$ kyr. In a similar fashion, we derive $M_{\rm init} = 1.5 \pm 0.5\ M_\odot$, $M_c = 0.60 \pm 0.04\ M_\odot$, $\tau_{\rm evol} \sim 70$ kyr from comparison with the He-burning tracks.

The derived stellar parameters of Lo 1 are similar to those of the hotter, higher gravity O(H) stars in the sample of central stars for old PN classified by Napiwotzki (1999). Thus, we confirm the Mèndez et al. (1985) classification of Lo 1 as a hgO(H) star.

Mèndez et al. (1985) performed a non-LTE analysis of its optical spectrum and obtained $T_{\rm eff} = 65 \pm 10$ kK, $\log g = 5.7 \pm 0.3$ cm s^{-2}, and $Y = 0.10 \pm 0.03$ for the central star. We have calculated a TLUSTY model with these parameters and find it fails to match the FUV data for multiple reasons. When this model is scaled to match the UV continuum level, it significantly underproduces the FUV continuum level. It also fails to duplicate many of the FUV diagnostics, most notably the strong O VI λλ1032, 1038 feature. Similarly, Hoare et al. (1996), from an analysis of the optical and extreme ultraviolet spectra of the CSPN NGC 1360, found a temperature significantly higher than the results of Mèndez et al. (1985), which were based on optical data only. Our significantly higher derived temperature and gravity illustrate the importance of considering the FUV wavelength regime when modeling such hot CSPN, where they emit the majority of their observable flux (i.e., longward of the Lyman limit) as well as display their strongest stellar features.

5. CONCLUSIONS

We have analyzed FUV and UV spectra of Lo 1, a hot CSPN notable for its relatively high galactic latitude and thus having a minimal reddening. Its *FUSE* spectrum, aside from showing hydrogen and helium lines, shows strong O VI λλ1032, 1038 signatures, perhaps indicating an oxygen-enriched object.

We have modeled the *FUSE* and *IUE* spectrum of this object to determine parameters $T_{\rm eff} = 120$ kK, $\log g = 6.7$ cm s^{-2}, $R_* = 0.04\ R_\odot$, $L = 250\ L_\odot$, and $M \simeq 0.6\ M_\odot$. The temperature is much higher than that derived by Mèndez et al. (1985) from an optical-line analysis ($T_{\rm eff} = 65 \pm 10$ kK), and illustrates the importance of the FUV–UV range in the analysis of hot CSPN. These parameters confirm the Mèndez et al. (1985) classification of Lo 1 as a high-gravity O(H) star. Comparison of our parameters to evolutionary tracks indicate a post-AGB age of ∼65 kyr. We also measure $v_{\rm rad} \simeq 100$ km s^{-1} for the Lo 1 PN system.

We thank Terry Lanz and Ivan Hubeny for their help with the TLUSTY code. We thank Stephan McCandliss for making his H_2 molecular data and tools available. We also are grateful to the referee, Klaus Werner, for his constructive comments. The SIMBAD database was used for literature searches. This work has been funded by NASA grant NAG 5-9219 (NRA-99-01-LTSA-029). The *IUE* data presented in this paper were obtained from the Multimission Archive (MAST) at the Space Telescope Science Institute (STScI). STScI is operated by the Association of Universities for Research in Astronomy, Inc., under NASA contract NAS 5-26555. Support for MAST for non-*Hubble Space Telescope* data is provided by the NASA Office of Space Science via grant NAG 5-7584 and by other grants and contracts.

REFERENCES

Anderson, L. S. 1989, ApJ, 339, 588
Bohlin, R. C., Savage, B. D., & Drake, J. F. 1978, ApJ, 224, 132
Cahn, J. H., Kaler, J. B., & Stanghellini, L. 1992, A&AS, 94, 399
Cunto, W., Mendoza, C., Ochsenbein, F., & Zeippen, C. J. 1993, A&A, 275, 5
Dreizler, S., & Werner, K. 1996, A&A, 314, 217
Grevesse, N., & Sauval, A. J. 1998, Space Sci. Rev., 85, 161
Hoare, M. G., Drake, J. J., Werner, K., & Dreizler, S. 1996, MNRAS, 283, 830
Hubeny, I. 1988, Comput. Phys. Comm., 52, 103
Hubeny, I., Hummer, D. G., & Lanz, T. 1994, A&A, 282, 157
Hubeny, I., & Lanz, T. 1992, A&A, 262, 501
———. 1995, ApJ, 493, 875
Hughes, M. P., Thompson, A. R., & Colvin, R. S. 1971, ApJS, 23, 323
Ishida, K., & Weinberger, R. 1987, A&A, 178, 227
Kaler, J. B., & Feibelman, W. A. 1985, ApJ, 297, 724
Kaler, J. B., & Lutz, J. H. 1985, PASP, 97, 700
Kohoutek, L., & Laustsen, S. 1977, A&A, 61, 761
Longmore, A. J. 1977, MNRAS, 178, 251
Mèndez, R. H., Kudritzki, R. P., & Simon, K. P. 1985, A&A, 142, 289
Moos, H. W., Cash, W. C., & Cowie, L. L. 2000, ApJ, 538, 1
Napiwotzki, R. 1997, A&A, 322, 256
———. 1999, A&A, 350, 101
Patriarchi, P., & Perinotto, M. 1991, A&AS, 91, 325
Sahnow, D. J., Moos, M. W., & Ake, T. B. 2000, ApJ, 538, 7
Vassiliadis, E., & Wood, P. R. 1994, ApJ, 92, 125
Werner, K. 1996, A&A, 309, 861
Werner, K., Heber, U., & Hunger, K. 1991, A&A, 244, 437
West, R. M., & Kohoutek, L. 1985, ApJS, 60, 91